

Proceedings of the Korean Nuclear Society Spring Meeting  
Gyeongju, Korea, May 2004

## Development of 3-D Multicomponent Mixture Analysis (GAMMA) Code for Pebble-Bed Safety Analysis in a HTGR

Hong Sik Lim

Korea Atomic Energy Research Institute  
150 Dukjin-dong, Yuseong-gu, Taejon, Korea 305-353  
hslim@kaeri.re.kr

Hee Cheon NO

Korea Advanced Institute of Science and Technology  
373-1 Guseong-dong, Yuseong-gu, Taejon, Korea 305-701  
hcno@nsys.kaist.ac.kr

### **Abstract**

We developed a multi-dimensional GAs Multicomponent Mixture Analysis (GAMMA) in order to investigate molecular diffusion, chemical reactions, and natural convection related to the air ingress phenomena during the primary-pipe rupture accident. In addition, GAMMA can handle the core thermal-hydraulic characteristics in a pebble bed-type gas cooled reactor. The Implicit Continuous Eulerian (ICE) technique is adopted for the reduction of  $10N \times 10N$  matrix into  $N \times N$  pressure difference matrix and fast transient computation. In the simulation of a SANA-1 afterheat self-removal test, the predicted results of GAMMA agree closely with the measured temperature profiles and are comparable to those of other analysis codes (TINTE, THERMIX, and TRIO-EF).

### **1. Introduction**

A High Temperature Gas cooled Reactor (HTGR) has the possibility, with a suitable design and dimensions, to meet the safety requirements for severe accidents. The afterheat, decay heat produced and stored heat in the core internal structures, is removed safely from the reactor core in a

hypothetical accident, the failure of all heat sinks after a reactor trip. Fuel temperature is not exceeded beyond the safety limit which leads to an increase of fission products release or a damage of the reactor structures. The heat in the core is transported at any time by the following possible mechanisms: heat conduction, radiation transfer, and natural convection. Since the afterheat is removed safely, no active means are required during the whole transient; however, this inherent feature should be confirmed using a reliable analysis code which is well verified and validated with experiments. In the view of thermal hydraulics, a pebble bed core poses several difficulties to accurately predict the temperature and flow fields: the boundary effects at the edge of a reactor core where the use of the effective thermal conductivity concept for a pebble bed cannot be justified, and existence of a geometric complexity by a mix of porous and non-porous regions. Therefore, the accurate determination of temperature distribution in the core is necessary to make sure that the pebble fuel temperature does not exceed the safety limit for all postulated accidents.

For the sake of investigating the thermal hydraulic characteristics under natural convection in a pebble bed, GAMMA has been validated with the SANA-1 heat removal test in a pebble bed.

## 2. Governing Equations and Numerical method

The multi-dimensional governing equations consist of the basic equations for continuity, momentum conservation, energy conservation of the gas mixture, and the mass conservation of each species. Six gas species (He, N<sub>2</sub>, O<sub>2</sub>, CO, CO<sub>2</sub>, and H<sub>2</sub>O) are considered. GAMMA has the capability to handle the thermal hydraulic and chemical reaction behaviors in a multicomponent mixture system as well as heat transfer within solid components, free and forced convection between solid and fluid, and radiation heat transfer between solid surfaces. As well, the basic equations are formulated using a porous media model that is effective in modeling a pebble bed-type HTGR.

### 2.1 Governing Equations

The field equations used in GAMMA are:

#### Continuity equation

$$\varphi \frac{\partial \rho}{\partial t} + \nabla \cdot (\rho \mathbf{u}) = \varphi \sum_s R_s \quad (1)$$

#### Momentum equation in a non-conservative form

$$\rho \left( \frac{1}{\varphi} \frac{\partial \mathbf{u}}{\partial t} + \frac{1}{\varphi^2} \mathbf{u} \cdot \nabla \mathbf{u} \right) = -\nabla P + \frac{1}{\varphi} \nabla \cdot (\mu \nabla \mathbf{u}) - \frac{\mu}{K} \mathbf{u} - \frac{C_F \rho}{\sqrt{K}} |\mathbf{u}| \mathbf{u} + \rho \mathbf{g} \quad (2)$$

Sensible energy equation for the fluid

$$\begin{aligned} \varphi \frac{\partial}{\partial t}(\rho H) + \nabla \cdot (\rho \mathbf{u} H) = \nabla \cdot [(\varphi \lambda_f + \lambda_{disp}) \nabla T_f] - \nabla \cdot \left( \varphi \sum_{s=1}^m H_s \mathbf{J}_s \right) - \varphi \sum_s \Delta h_{f_s}^o R_s \\ + h_{sf} a_{sf} (T_p - T_f) \end{aligned} \quad (3)$$

Species conservation equation

$$\varphi \frac{\partial}{\partial t}(\rho Y_s) + \nabla \cdot (\rho \mathbf{u} Y_s) = -\nabla \cdot (\varphi \mathbf{J}_s) + \varphi R_s \quad (4)$$

and for He,  $Y_m = 1 - \sum_{s=1}^{m-1} Y_s$

Equation of state for an ideal gas

$$\rho = \frac{P}{RT} \left( \sum_{s=1}^m Y_s / W_s \right)^{-1} \quad (5)$$

For a solid and a pebble bed, the same heat conduction equation is used. A thermal non-equilibrium model [1] is used to consider the heat exchange between fluid and pebbles for a porous medium as follows:

$$\left[ (1-\varphi)(\rho C)_p \right] \frac{\partial T_p}{\partial t} = \nabla \cdot (\lambda_{eff} \nabla T_p) + q'' - h_{sf} a_{sf} (T_p - T_f) \quad (6)$$

Radiation heat transfer in the enclosure is well-modeled by using an irradiation/radiosity method [2] which assumes that the fluid is non-participating and the radiation exchange between surfaces is gray and diffuse. The net radiation heat flux from agglomerated surface k, which consists of  $N_k$  faces of the original mesh, is given by

$$q_{rk}'' = \left[ \left( \sum_{j \neq k}^M F_{kj} \right) \varepsilon_k \bar{T}_k^4 - \varepsilon_k \sum_{j \neq k}^M F_{kj} J_j \right] \left[ \varepsilon_k + (1-\varepsilon_k) \sum_{j \neq k}^M F_{kj} \right]^{-1} \quad (7)$$

Physical properties, such as molar weight, viscosity, thermal conductivity, and sensible enthalpy, for each gas component and gas mixtures, are obtained from References 3 and 4.

## 2.2 Numerical Method

The governing equations are discretized in a semi-implicit manner in the staggered mesh layout and then dependent variables are linearized by the Newton method. For a fast computation, the Implicit Continuous Eulerian (ICE) technique [5] is adopted to reduce  $10N \times 10N$  matrix to  $N \times N$  pressure difference matrix. Due to the explicit treatment of the second order terms, GAMMA is subjected to restriction of time step size, limited by convective, diffusive, conductive, and viscous transport times. The heat conduction equation, Eq. (6), is solved by the Crank-Nicolson method and coupled explicitly

with the fluid thermal-hydraulic calculation.

### 3. Validation with the SANA-1 Afterheat Self-removal Test

For flow resistances in a packed bed, the Forchheimer-extended Darcy's law [1] with parameters recommended by the German safety guide KTA3102.3 [6] is used.

$$K = \frac{d_p^2 \phi^3}{160(1-\phi^2)} \text{ and } C_F = \frac{3}{\sqrt{160}\phi^{3/2}} \left( \frac{1-\phi}{\text{Re}_p} \right)^{0.1} \quad (9)$$

The effective thermal conductivity of the pebble bed is calculated from the cell model of Zehner/Bauer/Schlünder described in Reference 7. Figure 1 shows the calculated and measured effective thermal conductivity for a pebble bed. The boundary effects due to the variation of porosity near the wall, channeling and thermal dispersion [1], are considered as follows:

$$\begin{aligned} \phi &= \phi_\infty \left[ 1 + 1.4 \exp(-5y/d_p) \right] \\ (\lambda_{disp})_{yy} &= 0.12(\rho C)_f d_p (V_z) \left[ 1 - \exp(-y/d_p) \right], \quad (\lambda_{disp})_{xx} = (\lambda_{disp})_{zz} = (\lambda_{disp})_{yy} / 3 \end{aligned} \quad (10)$$

For the pebble-to-fluid heat transfer coefficient ( $h_{sf}$ ), the German safety guide KTA3102.2 [8] is used as follows:

$$h_{sf} = \frac{\lambda_f}{d_p} \left( 1.27 \frac{\text{Pr}^{1/3}}{\phi^{1.18}} \text{Re}_p^{0.36} + 0.033 \frac{\text{Pr}^{1/2}}{\phi^{1.07}} \text{Re}_p^{0.86} \right) \quad (11)$$

The SANA-1 self-acting afterheat removal tests [7], one of the IAEA benchmark problems, have been simulated to validate the porous media model that is incorporated into the GAMMA code. The SANA-1 test apparatus shown in Figure 2 consists of a cylindrical pebble bed having a diameter of 1.5 m and a height of 1 m, a central heating element, and bottom and top insulators. The pebble bed is filled with approximately 9500 graphite pebbles with diameters of 6 cm in irregular arrangement. In this experiment, various configurations and conditions were investigated as listed Table 1: different kinds of fluids (nitrogen and helium), pebble sizes (3 cm and 6 cm), heating conditions (uniform and non-uniform), and configurations with and without a gas plenum.

By using the information available from Reference 7, all the test cases have been simulated and the predicted results have been compared with those of other codes (TINTE: Germany, THERMIX: China, and TRIO-EF: France). Figure 2 shows the GAMMA axi-symmetric mesh scheme with 1000 meshes for the fluid region and 1440 meshes for the solid region including a pebble bed. Due to the rotational symmetry of the SANA-1 facility, the 2-D geometry model can be used and, since the amount of heat generated or removed from the heater element and the top and bottom coolers is known, heat fluxes can be used as boundary conditions.

Figure 3 shows the predicted temperature profiles at three layers for the long element heating case

at 30kW power. The radial temperature distributions are the highest in the upper layer and the lowest in the lower layer due to a clock-wise free convection flow. The relative temperature difference between the layers is larger with nitrogen as a filled-gas than with helium due to difference in specific heat. The predicted temperature profiles for the long element heating case at 10kW power shown in Figure 4 show similar trends with the previous high power case, but the temperature difference between layers becomes larger because of lower free convection flow.

For the non-uniform top-element heating case shown in Figure 5, there are differences among the calculated results from four analysis codes particularly in the lower layer. The differences may come from the use of the different values in the simulation of each code due to lack of accurate data for the heat removed from a bottom cooler. For the non-uniform bottom-element heating case shown in Figure 6, the radial temperature distributions are reversed, the highest in the lower layer and the lowest in the upper layer.

For the bottom-element heating case with a gas plenum above a pebble bed shown in Figure 7, we consider radiation exchange in the gas plenum. Therefore, the calculated temperature distribution near the radiating surface at 63 cm shows a satisfactory level of agreement with the measured data.

For the long element heating cases with 3 cm pebbles, Figures 8 and 9 show the predicted results for 30kW and 10kW power cases, respectively. The magnitude of temperatures is generally higher and the temperature difference between layers is lower, than those for 6 cm pebble due to smaller influence of the convective heat transport and lower effective thermal conductivity.

In all simulated cases, the prediction results of GAMMA agree closely with the measured temperature distributions and are comparable to other codes' results, although in some cases slight deviation is observed in the lower layer due to insufficient information on the heat removed from top and bottom coolers. Since the cell model of Zehner/Bauer/Schlünder underestimates the effective thermal conductivity for He as shown in Figure 1, the deviation from the experiment is larger for the He-filled case than for the N<sub>2</sub>-filled case.

#### **4. Conclusions**

In all simulated cases for a SANA-1 afterheat removal test, the prediction results of GAMMA agree closely with the measured temperature profiles and are comparable to those of other analysis codes (TINTE, THERMIX, and TRIO-EF). Since the cell model of Zehner/Bauer/Schlünder underestimates the effective thermal conductivity for He, the deviation from the experiment is larger for the He-filled case than for the N<sub>2</sub>-filled case. On the basis of theoretical model, it is necessary to further improve the effective thermal conductivity of the pebble bed and to elaborate on modeling the boundary effects at the edge of a reactor core.

## Nomenclature

$a_{sf}$	= specific surface area ( $m^{-1}$ )
$C_F$	= drag coefficient
$d_p$	= pebble diameter (m)
$F_{ij}$	= geometric view factor
$g$	= gravitational constant
$h_{sf}$	= pebble-to-fluid heat transfer coefficient ( $W/m^2-K$ )
$\Delta h_f^o$	= latent heat of formation for chemical reaction ( $J/kg$ )
$H$	= sensible enthalpy of gas mixture ( $J/kg$ )
$H_s$	= sensible enthalpy of species, s ( $J/kg$ )
$J_i$	= radiosity ( $W/m^2$ )
$\mathbf{J}_s$	= total diffusion flux w.r.t. mass average velocity ( $kg/m^2-s$ )
$K$	= permeability
$m$	= total number of species
$N$	= total number of computational meshes
$P$	= total pressure (Pa)
$Pr$	= Prandtl number
$q'''$	= volumetric heat source ( $W/m^3$ )
$q_r''$	= net radiation heat flux ( $W/m^2$ )
$\bar{R}$	= universal gas constant
$Re_p$	= Reynolds number based on pebble diameter
$R_s$	= generation/dissipation of species, s, by chemical reaction ( $kg/m^3-s$ )
$T_f$	= temperature of gas mixture (K)
$\bar{T}_k$	= temperature of agglomerated surface, k (K)
$T_p$	= solid or pebble temperature (K)
$\mathbf{u}$	= mass average velocity of fluid (m/s)
$W_s$	= molar weight of species, s (g/mol)
$y$	= distance from the rigid wall (m)
$Y_s$	= mass fraction of species, s

## Greek Symbols

$\rho$	= density of gas mixture ( $kg/m^3$ )
$\phi$	= porosity
$(\rho C)_f$	= volumetric heat capacity of fluid ( $J/m^3-K$ )

- $(\rho C)_p$  = volumetric heat capacity of pebble (J/ m<sup>3</sup>-K)  
 $\lambda_{disp}$  = thermal conductivity of fluid induced by thermal dispersion (W/m-K)  
 $\lambda_f$  = thermal conductivity of fluid (W/m-K)  
 $\lambda_{eff}$  = effective thermal conductivity of pebble bed (W/m-K)  
 $\mu$  = viscosity of fluid (kg/m-s)  
 $\sigma$  = Stefan Boltzmann constant

## References

- [1] D.A. Nield, A. Bejan, *Convection in Porous Media*, Springer-Verlag, New York, 1999.  
[2] J.P. Holaman, *Heat Transfer*, McGraw-Hill, 1986.  
[3] B.E. Poling, J.M. Prausnitz, J.P. O'connell, *The Properties of Gases and Liquids*, McGraw-Hill, 2001.  
[4] K. Raznjevic, *Handbook of Thermodynamic Tables and Charts*, Hemisphere, Washington, 1976.  
[5] F.H. Harlow, A.A. Amsden, "A Numerical Fluid Dynamics Calculation Method for All Flow Speeds," *J. Comp. Phy.*, Vol.8, p.197-213, 1971.  
[6] German Safety Guide KTA3102.3, German Nuclear Safety Standards Commission, 1981.  
[7] *Heat Transport and Afterheat Removal for Gas Cooled Reactors Under Accident Conditions*, IAEA-TECDOC-1163, Chap. 4.2, 2000.  
[8] German Safety Guide KTA3102.2, German Nuclear Safety Standards Commission, 1981.

Table 1. Experimental cases conducted in a SANA-1 test facility

Config uration	Pebble diameter (mm)	Heating tube/pebble bed geometry	Gas	Heating power (kW)
(1)	60	long heating element	N <sub>2</sub> , He	10, 30
(2)	60	short heating element at the top	N <sub>2</sub> , He	20
(3)	60	short heating element at the bottom	N <sub>2</sub> , He	20
(4)	60	short heating element at the bottom with gas plenum above the pebble bed	N <sub>2</sub> , He	20
(5)	30	long heating element	N <sub>2</sub> , He	10, 30

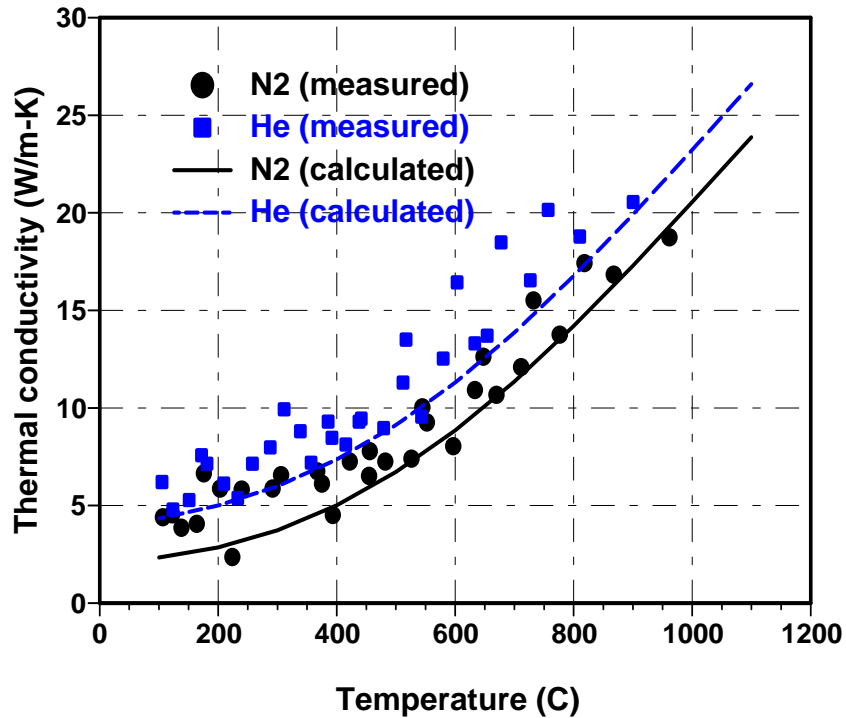


Fig. 1. Effective thermal conductivity of a pebble bed calculated by the cell-model of Zehner/Bauer/Schlünder

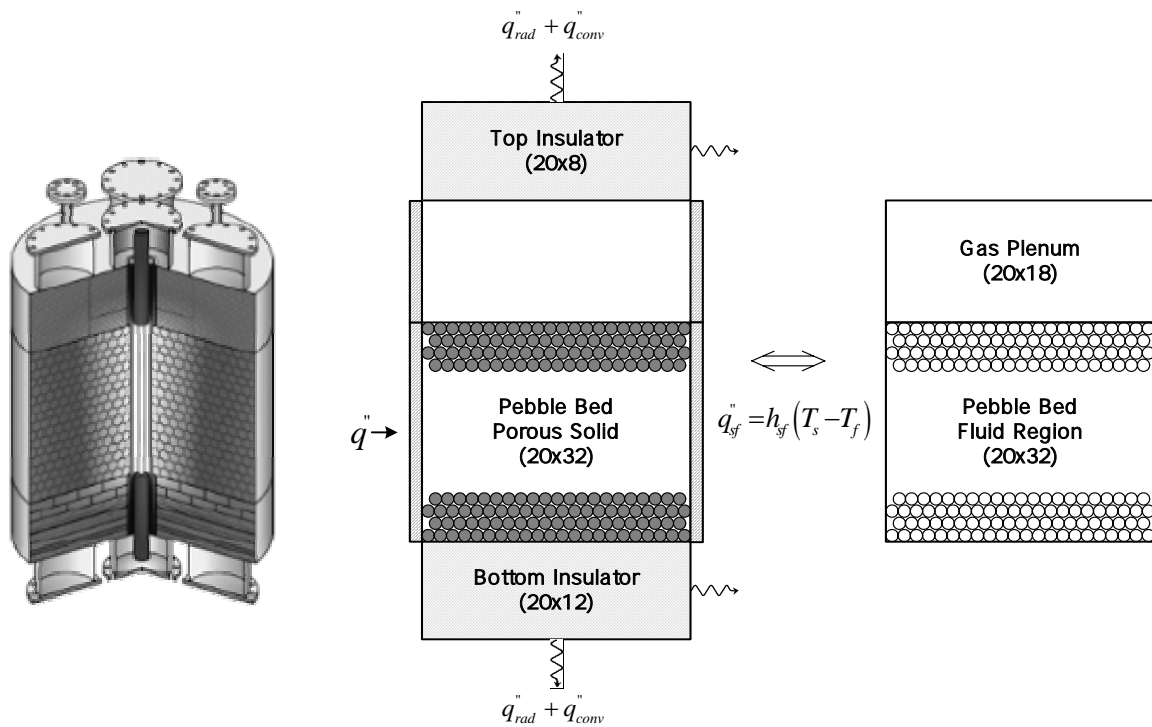


Fig. 2. SANA-1 test facility and GAMMA 2-D mesh scheme for the configuration (4) with a gas plenum above a pebble bed

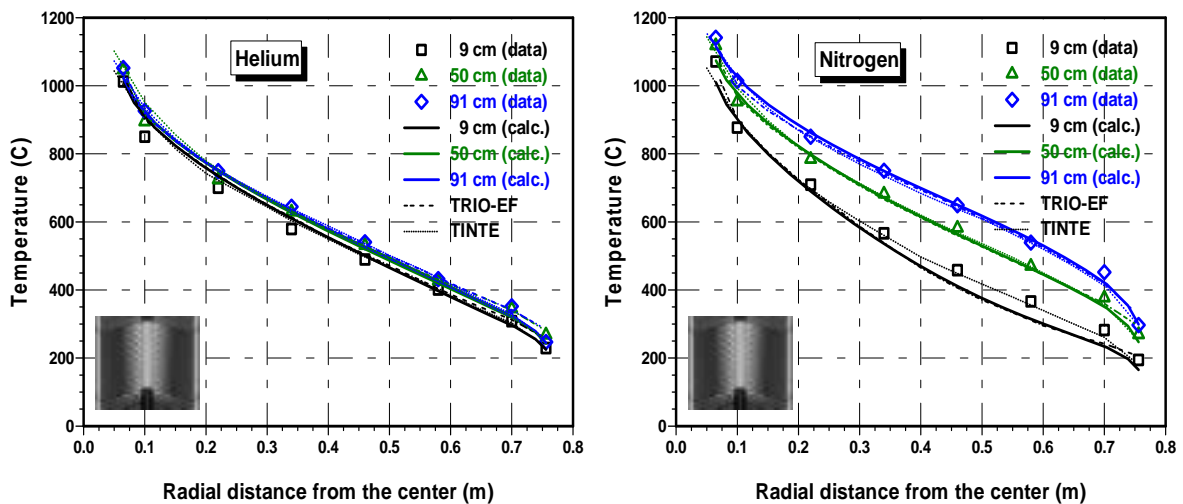


Fig. 3. Calculated and measured temperature distributions: long heating element, 30kW heating power, and 6 cm pebble

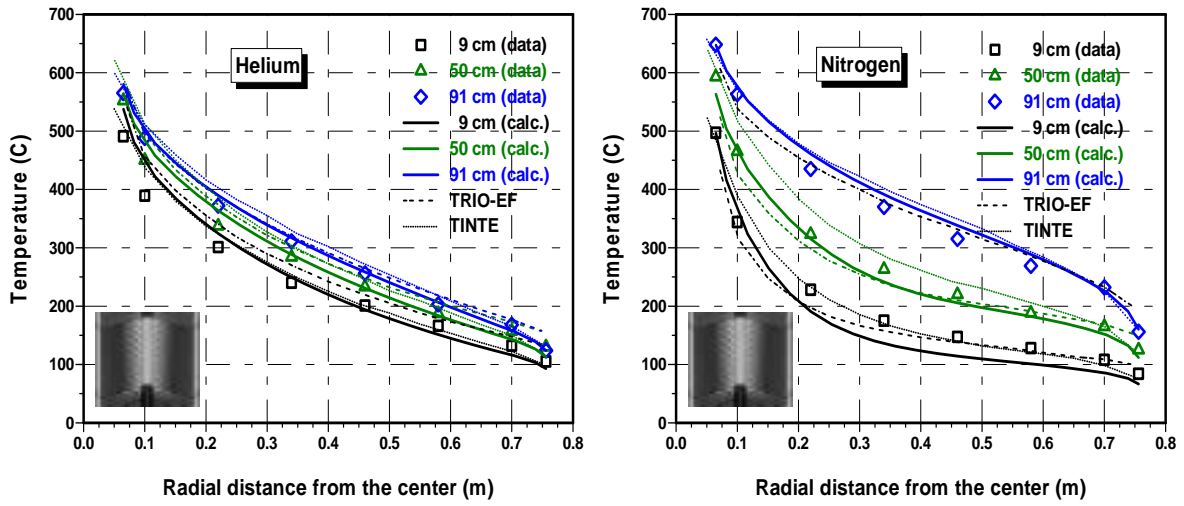


Fig. 4. Calculated and measured temperature distributions: long heating element, 10kW heating power, and 6 cm pebble

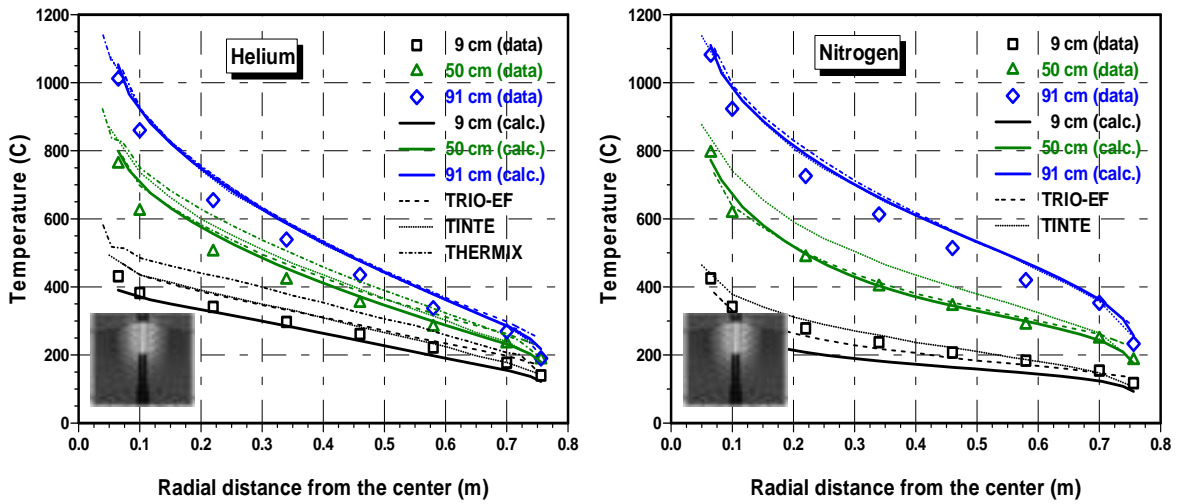


Fig. 5. Calculated and measured temperature distributions: short heating element at the top, 20kW heating power, and 6 cm pebble

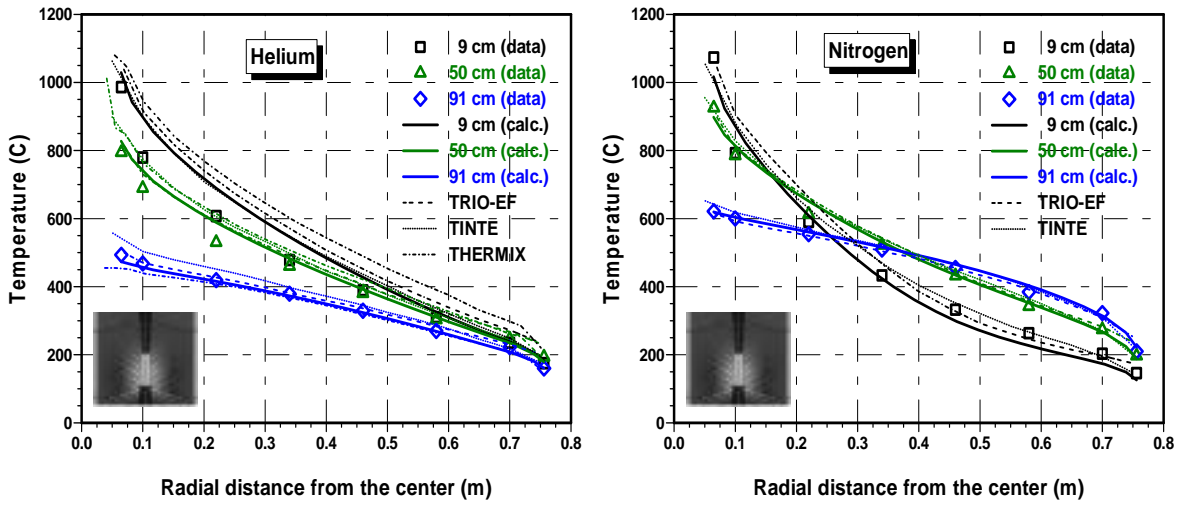


Fig. 6. Calculated and measured temperature distributions: short heating element at the bottom, 20kW heating power, and 6 cm pebble

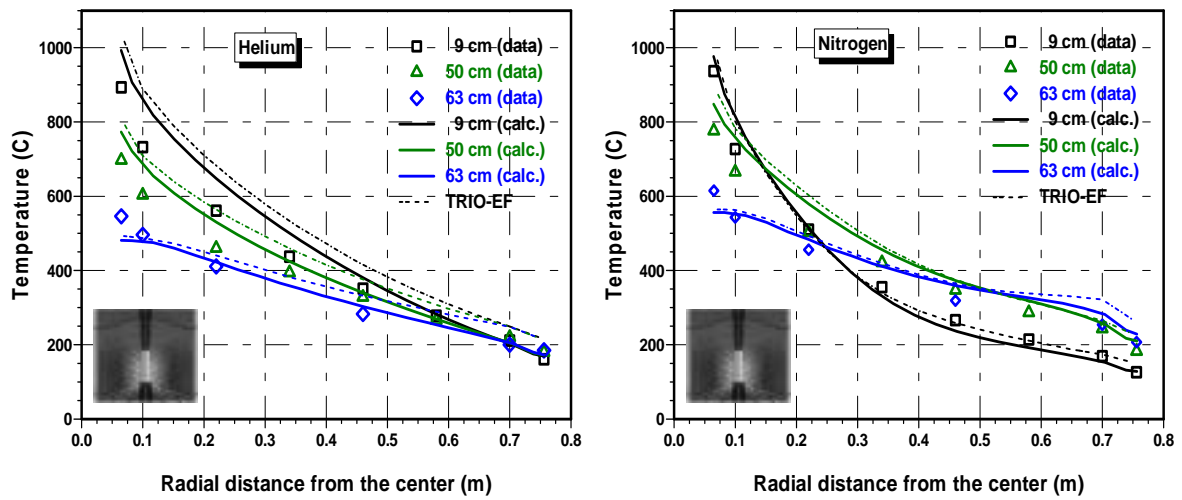


Fig. 7. Calculated and measured temperature distributions: short heating element at the bottom with a gas plenum, 20kW heating power, and 6 cm pebble

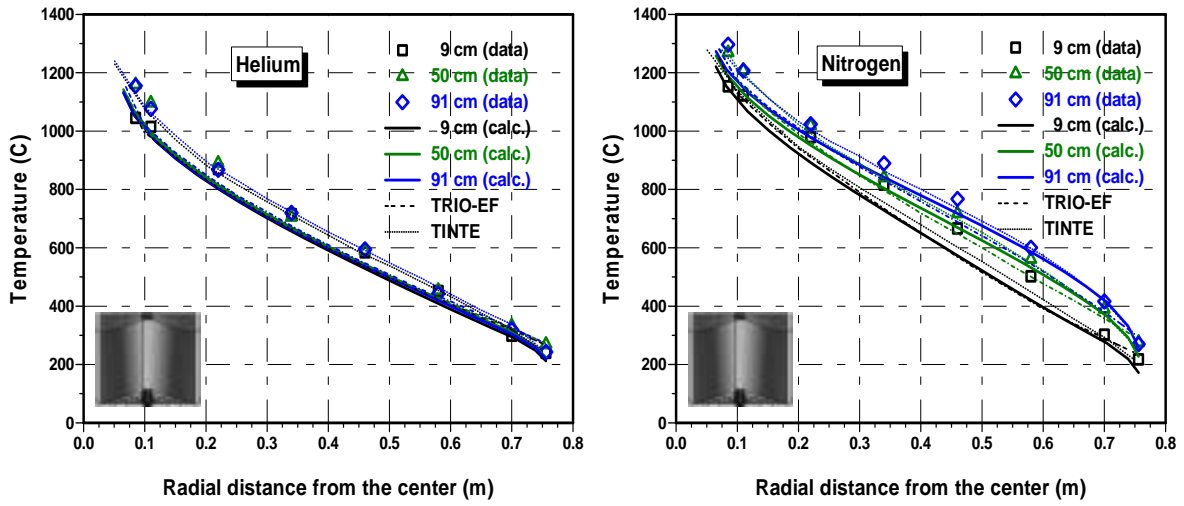


Fig. 8. Calculated and measured temperature distributions: long heating element, 30kW heating power, and 3 cm pebble

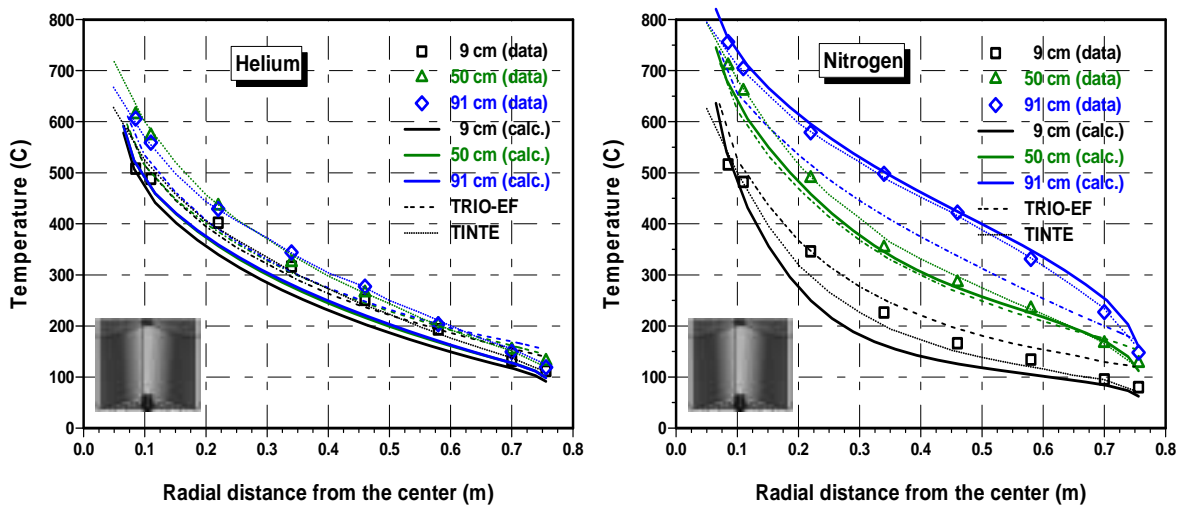


Fig. 9. Calculated and measured temperature distributions: long heating element, 10kW heating power, and 3 cm pebble